Drug designing against NSP15 of SARS-COV2 via high throughput computational screening and structural dynamics approach

Abida Batool [a], Nousheen Bibi [a,*], Farhat Amin [a], Mohammad Amjad Kamal [b,c,d]

[a] Department of Bioinformatics Shaheed Benazir Bhutto Women University, Peshawar, Pakistan
[b] King Fahd Medical Research Center, King Abdulaziz University, Jeddah, 21589, Saudi Arabia
[c] Enzymoics, 7 Peterlee Place, Hebersham, NSW, 2770, Australia
[d] Novel Global Community Educational Foundation, Australia

ARTICLE INFO

ABSTRACT

The rapid outbreak of the COVID-19 also known as SARS-CoV2 has been declared pandemic with serious global concern. As there is no effective therapeutic against COVID-19, there is an urgent need for explicit treatment against it. The focused objective of the current study is to propose promising drug candidates against the newly identified potential therapeutic target (endonuclease, NSP15) of SARS-CoV2. NSP15 is an attractive druggable target due to its critical role in SARS-CoV2 replication and virulence in addition to interference with the host immune system. Here in the present study, we integrated the high throughput computational screening and dynamic simulation approach to identify the most promising candidate lead compound against NSP15.5-fluoro-2-oxo-1H-pyrazine-3-carboxamide (favipiravir), (3R,4R, 5R)-3,4-Bis(benzyloxy)-5-((benzyloxy) methyl) dihydrofuran-2(3H)-one) remedesivir, 1,3-thiazol-5-ylmethyl N-[(2S,3S, 5S)-3-hydroxy-5-[[(2 S)-3-methyl-2-[[methyl-[(2-propan-2-yl-1,3-thiazol-4-yl)methyl]carbamoyl]amino]butanoyl]amino]-1,6-diphenylhexan-2-yl] carbamate (ritonavir), ethyl (3R,4R, 5S)-4-acetamido-5-amino-3-pentan-3-yloxycyclohexene-1-carboxylate (oseltamivir), and (2 S)–N-[(2S,4S, 5S)-5-[[2-(2,6-dimethylphenoxy)acetyl]amino]-4-hydroxy-1,6-diphenyl-hexan-2-yl]-3-methyl-2-(2-oxo-1,3-diazinan-1-yl)butanamide (lopinavir) were chosen as a training set to generate the pharmacophore model. A dataset of ~140,000 compounds library was screened against the designed pharmacophore model and 10 unique compounds were selected that passed successfully through geometry constraints, Lipinski Rule of 5, and ADME/Tox filters along with a strong binding affinity for NSP15 binding cavity. The best fit compound was selected for dynamic simulation to have detailed structural features critical for binding with the NSP15 protein.

Given our detailed integrative computational analysis, a Small molecule (3,3-Dimethyl-N-[4-(1-piperidinylcarbonyl) phenyl] butanamide) with drug-like properties and high binding affinity with the NSP15 is proposed as a most promising potential drug against COVID-19. The current computational integrative approach may complement high-throughput screening and the shortlisted small molecule may contribute to selective targeting of NSP15 to stop the replication of SARS-CoV2.

1. Introduction

In late 2019, the rapid outbreak of a novel coronavirus, named severe acute respiratory syndrome coronavirus 2 (SARS-CoV2) was found in Wuhan, China as a root cause for many cases of respirational ailment. Presumably, the virus instigated as a result of zoonotic transmission among animals like bats and humans but heap on by human to human through common droplet contagion (Wang et al., 2020; Li et al., 2020 and Sohrabi et al., 2020).

The virus hastily blowout starting from China to above 212 countries worldwide and, till this date, infested almost more than 3 million people, and over 0.2 million mortalities are reported (as of May 1, 2020) (https://www.who.int/emergencies/diseases/novel-coronavirus-2019/situation-reports). The World Health Organization (WHO) affirmed the SARS-CoV2 pandemic a Public Health Emergency of International Concern and gave the abbreviated name of COVID-19 to the SARS-CoV2 outbreak (Sohrabi et al., 2020, https://www.who.int/emergencies/diseases/novel-coronavirus-2019/events-as-they-happen).

---

* Corresponding author. Shaheed Benazir Bhutto Women University, Peshawar, Pakistan.
E-mail addresses: biogomal@gmail.com, drnosheenbibi@sbbwu.edu.pk (N. Bibi).

COVID-19 is capable of causing respiratory epidemics in humans like severe acute respiratory syndrome coronavirus 1 (SARS-CoV1) in 2002–2003 (Centers for Disease Control and Prevention, 2003) and Middle-East Respiratory Syndrome coronavirus (MERS CoV) in 2012 (de Wit et al., 2016). Based on the data of 2003 and 2012 epidemics of SARS-CoV1 and MERS-CoV, COVID-19 is considered the cause of great loss of human lives as well as it will exert massive social impact and economic loss in the billions of dollars (Stoermer et al., 2020; Keogh-Brown et al., 2008).

SARS CoV-2 is an enveloped non-segmented positive-sense RNA virus that belongs to the β-coronaviruses family. Its genome size is 29.9 kb (Wu et al., 2020). It has been discovered that the genome of β-coronaviruses consists of 6–11 open reading frames (ORFs) (Song et al., 2019). More than half part of viral RNA, found in the first ORF (ORF1a/b) decodes two polyproteins, pp1a and pp1ab, and encrypts 16 non-structural proteins (NSP), while the remaining ORFs translate auxiliary and structural proteins comprising spike (S) glycoprotein, small envelope (E) protein, matrix (M) protein, and nucleocapsid (N) protein (Cui et al., 2019). Recently, NSP15 is declared a suitable drug target against SARS-CoV2 as it is conserved among coronaviruses and is crucial for their lifecycle and virulence. It has been discovered that inhibition of NSP15 can slow viral replication more than any other target (https://news.northwestern.edu/stories/2020/03/new-coronavirus-protein-reveals-drug-target/). Among *Nidovirales* order, NSP15 is considered a genetic marker, differentiating it from all other viruses. The importance of NSP15 for virus structure is best illustrated in the work of Ivanov et al., in 2004 i.e. mutation in a single-nucleotide of NSP*15* demolished its endonucleolytic activity and viral RNA synthesis. Nsp15 plays a dominant role in suppressing the type I IFN (IFN-α/β)-associated innate immune response by infecting macrophages, thus eluding detection of viral mRNA by double-stranded RNA sensors. These interpretations have been auxiliary substantiated *in vivo* in murine models where virus expressing mutant nsp15 forms resulted in early forceful initiation of interferon, apoptosis of macrophages, and stimulated a protective immune response ultimately leading to attenuated disease. Therefore, this endonuclease can be considered as virus weakness and a highly specific and unique target for anti-CoV therapeutics (Senanayake, 2020).

At this moment in time, there is no specific drug or therapeutic option is available against COVID-19. Some already existing antiviral drugs have been ratified as an investigational remedy against COVID-19 like Favipiravir (Abou-Zeid, 2020, https://forum.facmedicine.com/threads/breaking-news-Favipiravir-approved-as-experimental-coronavirus-drug.47832/), Remedesivir, Chloroquine (Wang et al., 2020b), Ritonavir, Oseltamivir, and Lopinavir (https://www.dawn.com/news/1532081). Accordingly, there is still an exigent requirement for the development of an antiviral inhibitor specifically effective against COVID-19.

The present study was designed to use the computational approaches to design potential anti-viral lead compounds to defeat SARS-CoV2. We used these effective already existing drugs to propose the best inhibitor against COVID-19 by using Pharmacophore Modelling, Virtual Screening, Molecular Docking, and Molecular dynamic Simulation techniques. Expectantly, this research will add to uphold the existing efforts of the researchers to discover a certain cure against this dreadful virus.

2. Materials and methods

2.1. Data collection

The structure of NSP15 was obtained from PDB (https://www.rcsb.org/), with PDB ID: 6VWW (Kim et al., 2020). The crystal structure of NSP15 was further refined through energy minimization by Chimera 1.6.1 (http://www.rbvi.ucsf.edu/chimera) (Yang et al., 2012) using amber force field and geometry optimization by VEGA ZZ (http://www.

ddl.unimi.it). The 3D structure for training compound dataset containing favipiravir (CID: 492,405), remedesivir (CID: 121304016), ritonavir (CID: 392,622), oseltamivir (CID: 449,381), and lopinavir (CID: 92,727) were retrieved from the PubChem database (https://pubchem.ncbi.nlm.nih.gov/).

After this, we retrieved Antiviral Library (80,000 compounds), Antiviral HBV (11,000 compounds), Coronavirus Library (13,000 compounds) from ChemDiv (https://www.chemdiv.com/) and FDA approved drug library (1700 compounds) from Selleckchem (https://www.selleckchem.com/screening/fda-approved-drug-library.html). All drug libraries were retrieved in. sdf format. MONA 2.1.3 (Hilbig and Rarey, 2015) tool was used to remove redundancy among these libraries. Open Babel (O'Boyle et al., 2011) was used for format conversion of library compounds like from. sdf to. mol or. pdb and vice versa.

2.2. Pharmacophore modelling and virtual screening

The common featured ligand-based pharmacophore model for the training set of the molecules (Favipiravir, Remedesivir, Ritonavir, Oseltamivir, and Lopinavir) was created using Ligand Scout 4.3 (www.inteligand.com) (Amanlou and Mostafavi, 2017). Pharmacophore modelling is based on the assembly of chemical functionalities and then the alignment of shared features of the training compounds set. Then by resulted pharmacophore model sensitivity and specificity check was applied to optimize and refine the libraries of small molecules to find only active hits and eliminate the inactive hits from initial screening.

2.3. Virtual screening

The refined pharmacophore model was used as a query for virtual screening of the 0.14 million compounds of Antiviral, Antiviral HBV, Coronavirus, and FDA approved drug libraries using Ligand Scout 4.3. The basic key to success for the drug designing process is the enrichment of chemical database by which all the compounds with poor drug-like properties are removed and remaining filtered out hit molecules passes through a series of filters.

Initially, PAINS server (Baell and Holloway, 2010) was used to remove false positive hits, and then Osiris Property Explorer Applet (Dillard and Goldberg, 1978) (http://www.openmolecules.org/propertyexplorer/applet.html) and Osiris Data Warrior (Sander et al., 2015) (http://www.openmolecules.org/datawarrior/) were used to check Lipinski-filter (Lipinski, 2004) and geometry constraint from the screened compound. Through this enrichment process, we filtered out ~3500 compounds with optimized geometrical constraints, Mwt 180–450 kDa, LogP value of 1–5, five or fewer rotatable bonds, less than five hydrogen bond donors (HBD's), and less than ten hydrogen bond acceptors (HBAs). Moreover, SCIfinder (Ridley, 2009) was used to explore whether our active hits are previously reported in the literature, and also similarity search was done to assemble and inspect all those hits with> 80% similarity.

2.4. Molecular docking

The optimized screened compounds (~3500), with adequate pharmacological features, Lipinski filter, and geometrical constraints were kept to molecular docking studies in the active binding pocket of NSP15 of SARS-CoV 2. Auto Dock Vina wizard of PyRx (Dallakyan and Olson, 2015) was used to perform docking studies. Then docking complexes were crosschecked by using the Patch Dock server (Schneidman-Duhovny et al., 2005). Molecular docking was performed with a rigid receptor and flexible ligands. A grid map of 73 _ 21 _ 25 points with a spacing of 0.875 Å was set on the active binding pocket region of the NSP15 structure to create the grid map and remaining docking parameters were set to the default. The best-docked complex for each ligand was selected with the lowest energy value and interactions were checked using DS visualizer (Studio, 2008) and UCSF Chimera (Yang et al.,

2012).

2.5. ADME/tox properties

ADME-Tox (Absorption, Distribution, Metabolism, Excretion, and Toxicity) studies were conducted for the best interacting optimized screened compounds for Lead discovery and optimization. This pharmacokinetics, metabolism, and toxicity analysis is very important to predict the fate of Lead compounds after administration into the human body (Li, 2001). We used pkCSM (Pires et al., 2015) (http://biosig.un imelb.edu.au/pkcsm/) to check ADME/Tox for our compounds and then to crosscheck pharmacokinetics and ADME/Tox for best hit we used SwissADME (Daina et al., 2017) (http://www.swissadme.ch/). Hence, finally, we selected the best Lead compound passing Lipinski filter as well as ADME/Tox filter and has the best interaction with NSP15.

2.6. Molecular dynamic simulation

To examine the dynamic nature of interactions and to separate the comparative structural constraints between Apo and inhibitor bound states of NSP15, we performed molecular dynamics (MD) simulations for these two states. Molecular dynamics (MD) simulations were performed using MDWeb (Hospital et al., 2012) (http://mmb.irbbarcelona. org/MDWeb). In this GROMOS96 53a6 force field with the simple point charge (SPC) water model was used to simulate the protein complex. Erstwhile to the simulation process, energy minimization was performed by default using steepest descent and conjugate gradient methods, followed by equilibration under periodic boundary condition using octahedron box. MD simulation was performed for 100 ns under constant temperature (300 K) and pressure (1 ATM) and Particle-Mesh Ewald summation (Luty et al., 1994) was used to analyze electrostatic interactions. The steadiness of protein structure, fluctuations, and interactions was calculated by the root mean square deviation (RMSD) and root mean square fluctuations (RMSF) analysis.

3. Results

3.1. Pharmacophore model and virtual screening

The present study was designed to perform high throughput virtual screening extended with a structural dynamics approach to identify the potential candidate drug against NSP15. Ritonavir, remedesivir, oseltamivir, lopinavir, and favipiravir (Fig. S1) were used as a training set to generate the pharmacophore model. In an optimized model, their pharmacophore-fit score was 45.70, 47.48, 46.46, 48.14, and 46.09 respectively and they shared 4 common features i.e., each has two hydrogen bonds donors and two hydrogen bond acceptors. 2D and 3D view of the pharmacophore model are shown in Fig. 1 A and B. This model was used as a template for a screening of 140,000 compounds from Antiviral, Antiviral HBV, Coronavirus, and FDA approved drug

libraries. By the end of this screening process, we got ~3500 compounds with shared featured same as the pharmacophore model. We further screened out these 3500 compounds by removing false positive and by taking Lipinski rule of five and geometry constraints as standard. ~500 compounds were shortlisted. These ~500 compounds were in full agreement with pharmacophore features, geometry constraints, and Lipinski Rule of 5.

3.2. Lead selection through molecular docking and ADME/Tox analysis

To investigate the critical interactions with key residues of active binding sites of NSP15 protein of SARS-CoV2, an improved dataset of 500 compounds was subjected to molecular docking studies against the active binding pocket of NSP15 protein of SARS-CoV2. Docking analysis resulted in 50 docked inhibitors with strong binding affinities towards NSP15 protein (Table S1). A comparative docking analysis by Patch Dock (https://bioinfo3d.cs.tau.ac.il/PatchDock/) showed consistency in the docking poses and mapped residual interactions. Afterward, the chemistry of each compound was precisely evaluated and adjacent analogues and isomers were omitted. Finally, 10 unique compounds were selected for further analysis that showed a strong binding affinity for the NSP15 active site (Table 1). Lys71, Lys90, Gly165, Val166, Leu168, Thr196, Ser198, Arg199, Glu203, His 235, His 250, Leu252, Asp268, Asp273, Ser274, Lys277, Tyr279, Lys 290, Ser 294, Val295, Ile296, Asp297, Thr341 and Tyr343 of NSP15 were involved in the interaction with the 10 shortlisted compounds (Table S2).

By synergy of molecular docking and pharmacokinetics results analysis (3,3-Dimethyl-N-[4-(1-piperidinylcarbonyl) phenyl] butanamide) a compound from Coronavirus Library with ID:13,729 was isolated as best among all 10 shortlisted (Tables 1 and 2) for detailed interaction and dynamics simulation analysis. 2D and 3D structure of potential potent NSP15 inhibitor are shown in Fig. 2 A and B.

3,3-Dim l-N-[4-(1-piperidinylcarbonyl)phenyl]butanamide was docked pretty well within the binding cavity of NSP15 with the binding free energy of −10.5 kcal/mol. Lys90, Asp273, and Lys277 showed tight π-π stacking interactions, Leu252 and Lys277 was part of alkyl and Pi-

Table 1
Binding energies of 10 shortlisted compounds.

S.No	Library name_number	Binding energy Kcal/mol
1	Antiviral HBV Library_2340	−9.0
2	Antiviral HBV Library_2970	−9.0
3	Antiviral HBV Library_7636	−9.2
4	FDA approved drug library_144	−9.8
5	FDA approved drug library_617	−9.3
6	FDA approved drug library_1349	−9.0
7	CORONAVIRUS Library_748	−9.5
8	CORONAVIRUS Library_8981	−9.5
9	CORONAVIRUS Library_13,710	−9.3
10	**CORONAVIRUS Library_13,729**	**−10.5**
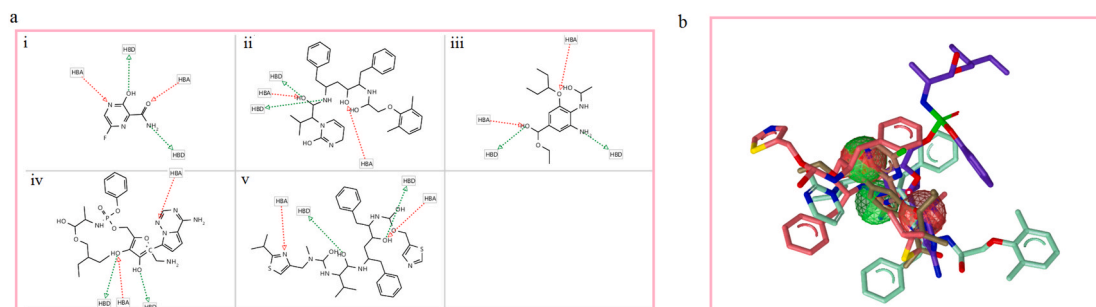
Fig. 1. 2D and 3D representation of the pharmacophore model. (A) 2D view of Pharmacophore. (i) Favipiravir (ii) Lopinavir (iii) Remedesivir (iv) Oseltamivir and (v) Ritonavir, respectively. B) 3D view of the Pharmacophore model.

Table 2
Pharmacokinetics properties of final screening hit.

Properties	Lead Compound
IUPAC Name	3,3-Dimethyl-N-[4-(1-piperidinylcarbonyl) phenyl]butanamide
Molecular Formula	$C_{18}H_{26}N_2O_2$
Canonical SMILES	O=C(CC(C) (C)C)Nc1ccc (cc1)C (=O)N1CCCCC1
Molecular Weight	302.41
LogP	3.68
Rotatable bonds	6
HBA	2
HBD	1
Molar Refractivity	93.84
Topological Polar Surface Area (TPSA)	49.41 $Å^2$
Surface Area	132.438
Water Solubility	−4.334/Soluble
ESOL Class Solubility	Soluble
Silicos-IT Class Solubility	Soluble
Ali Class Solubility	Soluble
Caco 2 permeability	1.363
Intestinal absorption (human)	90.495
Skin Permeability	−2.974
Gastrointestinal (GI) absorption	High
BBB permeant	Yes
CNS permeant	No
Pgp substrate	No
CYP1A2 inhibitor	No
CYP2C19 inhibitor	Yes
CYP2C9 inhibitor	No
CYP2D6 inhibitor	Yes
CYP3A4 inhibitor	No
Renal OCT2 substrate	Yes
AMES toxicity	No
Hepatotoxicity	No
Skin Sensitisation	No
Lipinski violations	0
Ghose violations	0
Veber violations	0
Egan violations	0
Muegge violations	0
Bioavailability Score	0.55
PAINS alerts	0
Brenk alerts	0
Leadlikeness violations	0
Synthetic Accessibility	1.89
DrugLikeness	Best
Medicinal Chemistry	Best

alkyl interactions while Ser198 and Lys71 were involved in hydrogen-bonding with important structural moieties of identified novel potent NSP15 inhibitor. Apart from this Gly165, Val166, Leu168, Thr196, Arg199, Glu203, Asp268, Ser274, Tyr279, Val295, Ile296, Asp297 showed hydrophobic interactions to keep the 3,3-Dimethyl-N-[4-(1-piperidinylcarbonyl) phenyl] butanamide pretty well within the binding pocket of the target protein (Fig. 3 A and B).

3.3. Molecular dynamic simulation analysis

To gauge stability, convergence, energetic and structural properties, 20 ns MD simulation was performed with selected putative lead compound and NSP15 of SARS-CoV2. Resulting trajectories were cautiously analysed to determine the stability, energetics, and structural properties and interactions during MD simulations.

Plots of root mean square deviation (RMSD) and root mean square fluctuation (RMSF) were generated to assess the stability and fluctuations. RMSD profile for bound NSP15 (NSP15-screening hit) was compared with the apo-state (NSP15) as a reference. An overall convergence of energies indicated well-behaved behaved-systems with equilibration. The RMSD plot shows values between the C-alpha atom of complex and apo-proteins were below 2 Å, signifying the system stability (Fig. 4A). RMSD plot verified more binding stability in NSP15 when it is bound to lead compound. These results strengthened our docking results as they were in good agreement with each other.

RMSF plot (Fig. 4B) indicated more fluctuations in the apo-state (NSP15). Interestingly, all fluctuations observed in apo-state were in the binding regions (in and around the binding residues i.e. (Lys71, Lys90, Ser198, and Leu252) and almost all binding residues persisted stability in complex form. These data specified that lead binding persuaded more compaction in the NSP15.

By thorough analysis of dynamic trajectories at different ns conformational changes in NSP15 binding cavity were captured most likely to critical for binding with the potential NSP15 inhibitor. Through the comparative analysis of NSP15 apo and NSP15 bound state, significant conformational changes were observed in the loop region and secondary structure surrounding the binding cavity while the residues involved in the binding showed stability except small conformational switches to facilitate binding with the inhibitor. Lys 252 and Lys277 tilted towards the cavity to make tight π-π stacking interaction and Pi-alkyl interaction with the bound inhibitor while Lys 71 and ser 198 showed inward push to make H-bonding with the inhibitor. Apart from these significant fluctuations in the loop region surrounding the binding residues were observed to help key residues to attain favourable binding pose (Fig. 5).

4. Discussion

Currently, COVID19 has been proved the most threatening and most frightening epidemic of this century so far. And most alarming is the fact that still there is no therapeutic available against this disease. In vitro process of drug designing that includes screening and testing of millions of compounds is time-consuming and very costly. The lack of explicit therapeutics against the novel COVID-19 urge for the active drug discovery for which computational methods offer a fast and cost-efficient
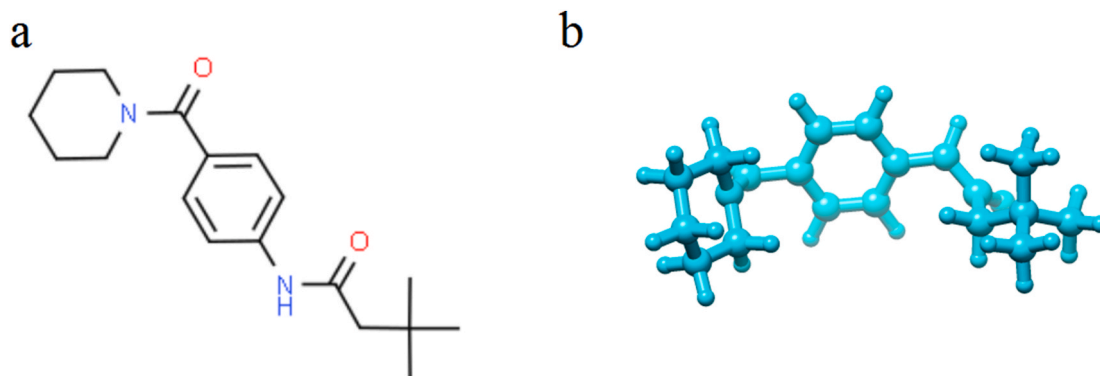

Fig. 2. 2D (a) and 3D (b) view of screening hit (3, 3-Dimethyl-N-[4-(1-piperidinylcarbonyl) phenyl] butanamide).
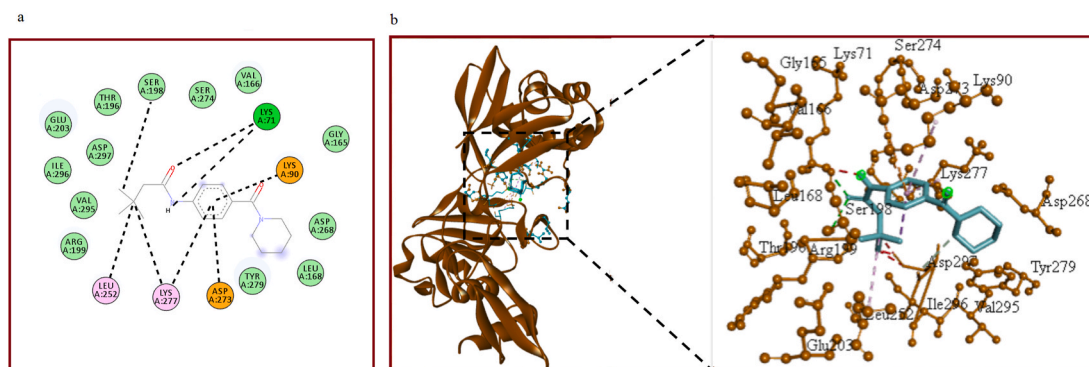
Fig. 3. Molecular interaction analysis of screening hit within the binding cavity of NSP15 protein. (A) 2D representation, a ligand is shown in the grey line model while the interacting residues are shown in discs. Black lines represent pi-pi and H-bonding interactions. (B) 3D representation, NSP15 protein is shown in brown ribbon with interacting residues shown in ball and stick representation Bound inhibitor molecule is shown in cyan stick model.
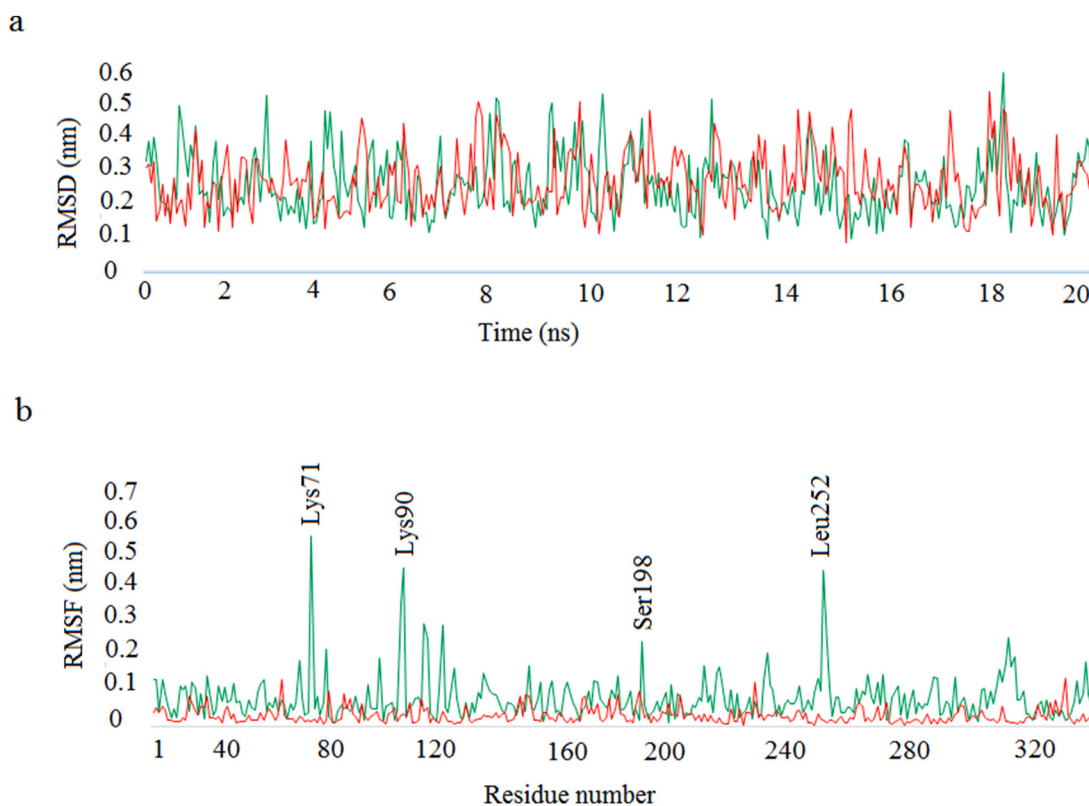

Fig. 4. Plots to investigate the stability and fluctuations of NSP15 apo and NSP15 bound state (**A**) Represents RMSD and (**B**) represents the RMSF plot. Green color represents the apo form of NSP15 while red color shows NSP15 bound with selected screening hit.

approach (Murumkar et al., 2010).

The present study was designed to use high throughput computational screening and structural dynamics approach to find out putative inhibitor against NSP15 protein of SARS-CoV-2. NSP15 that is considered vital for the SARS CoV-2 life cycle and virulence is declared as a new and effective drug target by a team of researchers from the University of California and the University of Chicago, North-western University. The team mapped the 3D structure of NSP15 (PDB ID: 6VWW) recently in march 2020 (Abou-Zeid, 2020; Kim et al., 2020). For drug designing, the information of a binding pocket of a receptor to its ligand is very crucial (Chou, 2006). The information about the binding cavity and residues involved in it was taken from Kim et al. (2020) and Abou-Zeid (2020). To increase the inhibition specificity, we integrated the pharmacophore modelling with virtual screening and dynamics simulations approach. Before designing pharmacophore model, five

training set of molecules (ritonavir, remedesivir, oseltamivir, lopinavir, and favipiravir) were evaluated for molecular interactions with the NSP15. Detailed interaction analysis revealed the strong binding affinity of all the training molecules within the active binding cavity with a number of covalent and hydrophobic interactions (Fig. S2). Comparative binding motif preference analysis with the target proteins of training molecules revealed preference of certain amino acid e. g Ser, Asp for Favipiravir (Sada et al., 2020), Gly, Asp for Lopinavir (Pal et al., 2013), Arg, Ser, Tyr for Oseltamivir (Karthick et al., 2013), Ser for Remedesivir (Lo et al., 2020), Arg, Asn and Ser for Ritonavir (Zhang and Yap, 2004). Binding analysis of these training compounds against NSP15 revealed the preference for those specific amino acids (Fig. S2).

Initially, by using 5 compounds (ritonavir, remedesivir, oseltamivir, lopinavir, and favipiravir) that showed positive therapeutic potential for coronavirus patients in different countries, a pharmacophore model was
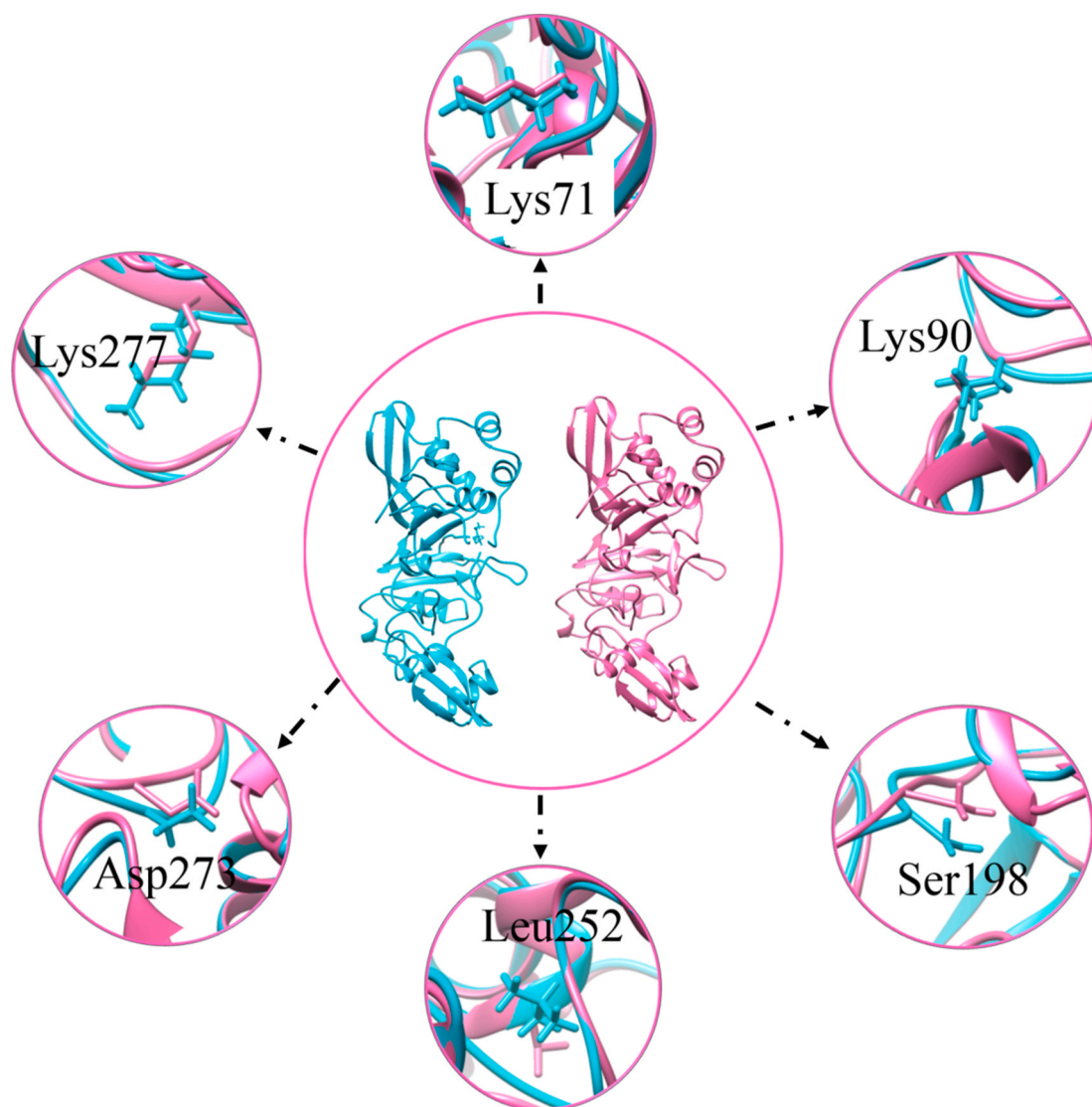
Fig. 5. Conformational changes of NSP15 upon inhibitor binding: Apo-state of NSP15 (pink) and bound sate of NSP15 (cyan) reveal critical structural changes upon inhibitor binding within the NSP15 binding pocket.

generated. The generated pharmacophore model was screened against a small molecule dataset of 140,000 compounds with subsequent filtration to increase specificity, resulting in the isolation of 10 hits as putative NSP15 specific inhibitors.

Finally, 3,3-Dimethyl-N-[4-(1-piperidinylcarbonyl) phenyl] butanamide was selected for detailed structural demonstration as representative screening hit for specific targeting of NSP15 protein of SARS-CoV2 (Table S3 and S4). Docking analysis reveals that along with Ser198, Lys71, Lys90, Arg199, Leu252, and Tyr279 are also more critical residues in the binding cavity of NSP15 (Fig. S2).

Detailed scrutinization of the dynamic behaviour of the final screening hit revealed important structural details of NSP15 binding pocket upon binding to lead compound. Comparative analysis of apo-state and inhibitor bound NSP15 complex uncovered significant structural compactness that may prove crucial to disrupting the SARS-CoV-2 virulence in the human body. During MD simulations, key substrate interacting residues (Lys71, Lys90, Ser198, and Leu252) were mainly detected in inhibitor binding which showed that isolated screening hot ma has a strong affinity towards the binding cavity of NSP15 (Fig. 4a and b). Therefore, detailed structural behavior monitoring strengthens our screening approach as NSP15 protein showed more stability in behavior upon binding to a putative inhibitor molecule. Our binding analysis with

our pharmacophore compounds strengthens our selection of lead compounds by exactly fitting within the same cavity.

Given our results analysis, we propose that our lead compound may prove more effective and specific for NSP15 targeted therapy. Our lead compound i.e. 3,3-Dimethyl-N-[4-(1-piperidinylcarbonyl) phenyl] butanamide is a small molecule with highly positive features of drug-likeness and Medicinal Chemistry can be the best potential drug against SARS-CoV2 inhibition, and it can be used with confidence for further in vitro analysis to investigate it with prospective of medicinal use.

5. Conclusion

To this date, no specific drugs or vaccines are available to treat SARS-CoV2 despite its close relation to the SARS-CoV1 virus that caused a similar epidemic in 2003. Thus, there remains a burning need for the development of specific antiviral therapeutics to conquer SARS-CoV2. The present study synergetic computational approach of virtual screening, molecular docking, and structural dynamics aimed to identify the potential NSP15 specific inhibitor from a library of 140,000 compounds. Out of shortlisted 10 compounds, (3,3-Dimethyl-N-[4-(1-piperidinylcarbonyl) phenyl] butanamide) exhibited strong interactions

within the binding cavity of NSP15 with the high binding free energy of −10.5 kcal/mol and stability within the binding site residues of NSP15.

To the best of our knowledge, A screening of a large set of chemical space for SARS-CoV2 endonuclease inhibitors has not been reported before. But we cannot eliminate the importance of in vitro or experimental validation to address the worthiness of our data. The immediate benefit of such studies is that they are needed for updating the treatment strategy for COVID-19. However, the targeted end-users of the expected results of the proposed study are drug manufacturing industries, clinicians, and subsequently the patients suffering from COVID-19.

Funding

Availability of data and material

The data supporting the findings of the article is available in the Protein Data Bank (PDB) at http://www.rcsb.org and PubChem database at https://pubchem.ncbi.nlm.nih.gov/.

CRediT authorship contribution statement

Abida Batool: Writing - original draft, performed experiment and manuscript writeup. **Nousheen Bibi:** Writing - original draft, Conceived and designed the study and write manuscript. **Farhat Amin:** made a substantial contribution in revising the manuscript for intellectual content. **Mohammad Amjad Kamal:** made a substantial contribution in revising the manuscript for intellectual content.

Declaration of competing interest

The authors declare no conflict of interest, financial or otherwise.

Appendix A. Supplementary data

Supplementary data to this article can be found online at https://doi.org/10.1016/j.ejphar.2020.173779.

References

Abou-Zeid, L., 2020, March 15. In Silico #Favipiravir Isostere a Promising Remedy: Lead Discovery for Covid-19 Recovery. Laila A Abou-Zeid; Associate Professor. FOP, Delta University & Mansoura University. https://doi.org/10.31219/osf.io/myw67.

Amanlou, M., Mostafavi, S.M., 2017. In silico screening to aim computational efficient inhibitors of caspase-9 by ligand-based pharmacophore modelling. J. Med. Biotech. 1 (1), 34–41. https://doi.org/10.22034/MBT.2017.60337.

Baell, J.B., Holloway, G.A., 2010. New substructure filters for removal of pan assay interference compounds (PAINS) from screening libraries and for their exclusion in bioassays. J. Med. Chem. 53 (7), 2719–2740. https://doi.org/10.1021/jm901137j.

2003 Centers for Disease Control and Prevention (CDC, 2003, 22. Update: Severe Acute Respiratory Syndrome–United States MMWR (Morbidity and Mortality Weekly Report), vol. 52, p. 525. PMID: 12803200.

Chou, K.C., 2006. Structural bioinformatics and its impact to biomedical science and drug discovery. Front. Med. Chem. 455 (502), 455–502.

Cui, J., Li, F., Shi, Z.L., 2019. Origin and evolution of pathogenic coronaviruses. Nat. Rev. Microbiol. 17 (3), 181–192. https://doi.org/10.1038/s41579-018-0118-9.

Daina, A., Michielin, O., Zoete, V., 2017. SwissADME: a free web tool to evaluate pharmacokinetics, drug-likeness and medicinal chemistry friendliness of small molecules. Sci. Rep. 7, 42717. https://doi.org/10.1038/srep42717.

Dallakyan, S., Olson, A.J., 2015. Small-molecule library screening by docking with PyRx. Chem. Biol. 243–250. https://doi.org/10.1007/978-1-4939-2269-7_19.

De Wit, E., Van Doremalen, N., Falzarano, D., Munster, V.J., 2016. SARS and MERS: recent insights into emerging coronaviruses. Nat. Rev. Microbiol. 14 (8), 523. https://doi.org/10.1038/nrmicro.2016.81.

Dillard, C.R., Goldberg, D.E., 1978. Chemistry: Reactions, Structure, and Properties. Macmillan, NY. USA, pp. 391–393.

Hilbig, M., Rarey, M., 2015. Mona 2: a light cheminformatics platform for interactive compound library processing. J. Chem. Inf. Model. 2071–2078. https://doi.org/10.1021/acs.jcim.5b00292.

Hospital, A., Andrio, P., Fenollosa, C., Cicin-Sain, D., Orozco, M., Gelpí, J.L., 2012. MDWeb and MDMoby: an integrated web-based platform for molecular dynamics

simulations Bioinformatics. https://doi.org/10.1093/bioinformatics/bts139, 28, 9, 1278-1279.

Ivanov, K.A., Hertzig, T., Rozanov, M., Bayer, S., Thiel, V., Gorbalenya, A.E., Ziebuhr, J., 2004. Major genetic marker of nidoviruses encodes a replicative endoribonuclease. Proc. Natl. Acad. Sci. U.S.A. 101 (34), 12694–12699. https://doi.org/10.1073/pnas.0403127101.

Karthick, V., Shanthi, V., Rajasekaran, R., Ramanathan, K., 2013. In silico analysis of drug-resistant mutant of neuraminidase (N294S) against oseltamivir Protoplasma. https://doi.org/10.1007/s00709-012-0394-6, 250, 1, 197-207.

Keogh-Brown, M.R., Smith, R.D., 2008. The economic impact of SARS: how does the reality match the predictions? Health Pol. 88 (1), 110–120. https://doi.org/10.1016/j.healthpol.2008.03.003.

Kim, Y., Jedrzejczak, R., Maltseva, N.I., Wilamowski, M., Endres, M., Godzik, A., Michalska, K., Joachimiak, A., 2020. Crystal structure of Nsp15 endoribonuclease NendoU from SARS-CoV-2. Protein Sci. https://doi.org/10.1002/pro.3873.

Li, A.P., 2001. Screening for human ADME/Tox drug properties in drug discovery. Drug Discov. Today 6 (7), 357–366. https://doi.org/10.1016/S1359-6446(01)01712-3.

Li, Y., Zhao, R., Zheng, S., Chen, X., Wang, J., Sheng, X., Zhou, J., Cai, H., Fang, Q., Yu, F., Fan, J., Xu, K., Chen, Y., Sheng, J., 2020. Lack of vertical transmission of severe acute respiratory syndrome Coronavirus 2, China. Emerg. Infect. Dis. 26 (6), 1335–1336. https://doi.org/10.3201/eid2606.200287.

Lipinski, C.A., 2004. Lead- and drug-like compounds: the rule-of-five revolution. Drug Discov. Today Technol. 1 (4), 337–341. https://doi.org/10.1016/j.ddtec.2004.11.007.

Lo, M.K., Albariño, C.G., Perry, J.K., Chang, S., Tchesnokov, E.P., Guerrero, L., Chakrabarti, A., Shrivastava-Ranjan, P., Chatterjee, P., McMullan, L.K., Martin, R., Jordan, R., Götte, M., Montgomery, J.M., Nichol, S.T., Flint, M., Porter, D., Spiropoulou, C.F., 2020. Remdesivir targets a structurally analogous region of the Ebola virus and SARS-CoV-2 polymerases. Proc. Natl. Acad. Sci. Unit. States Am. 117 (43), 26946–26954. https://doi.org/10.1073/pnas.2012294117.

Luty, B.A., Davis, M.E., Tironi, I.G., Van Gunsteren, W.F., 1994. A comparison of particle-particle, particle-mesh and ewald methods for calculating electrostatic interactions in periodic molecular systems. Mol. Simulat. 14 (1), 11–20. https://doi.org/10.1080/08927029408022004.

Murumkar, P.R., Zambre, V.P., Yadav, M.R., 2010. Development of predictive pharmacophore model for in silico screening, and 3D QSAR CoMFA and CoMSIA studies for lead optimization, for designing of potent tumor necrosis factor alpha converting enzyme inhibitors. J. Comput. Aided Mol. Des. 24 (2), 143–156. https://doi.org/10.1007/s10822-010-9322-z.

O'Boyle, N.M., Banck, M., James, C.A., Morley, C., Vandermeersch, T., Hutchison, G.R., 2011. Open babel: an open chemical toolbox. J. Cheminf. 3 (1), 33. https://doi.org/10.1186/1758-2946-3-33.

Pal, S., Mishra, M., Sudhakar, D.R., Siddiqui, M., 2013. In-silico designing of a potent analogue against HIV-1 Nef protein and protease by predicting its interaction network with host cell proteins. J. Pharm. BioAllied Sci. 5 (1), 66. https://doi.org/10.4103/0975-7406.106572.

Pires, D.E.V., Blundell, T.L., Ascher, D.B., 2015. pkCSM: predicting small-molecule pharmacokinetic and toxicity properties using graph-based signatures. J. Med. Chem. 58 (9), 4066–4072. https://doi.org/10.1021/acs.jmedchem.5b00104.

Ridley, D.D., Information Retrieval: SciFinder John Wiley & Sons, 2009. Rolling updates on corona-virus disease., 2020 rolling updates on corona-virus disease (COVID-19) march 20, 2020. https://www.who.int/emergencies/diseases/novel-coronavirus-2019/events-as-they-happen.

Sada, M., Saraya, T., Ishii, H., Okayama, K., Hayashi, Y., Tsugawa, T., Kimura, H., 2020. Detailed molecular interactions of favipiravir with SARS-CoV-2, SARS-CoV, MERS-CoV, and influenza virus polymerases in silico. Mic. Org. 8 (10), 1610. https://doi.org/10.3390/microorganisms8101610.

Sander, T., Freyss, J., Von Korff, M., Rufener, C., 2015. Data Warrior: an open-source program for chemistry aware data visualization and analysis. J. Chem. Inf. Model. 55 (2), 460–473. https://doi.org/10.1021/ci500588j.

Schneidman-Duhovny, D., Inbar, Y., Nussinov, R., Wolfson, H.J., 2005. PatchDock and SymmDock: servers for rigid and symmetric docking. Nucleic Acids Res. 33 (Suppl. l_2), W363–W367. https://doi.org/10.1093/nar/gki481.

Senanayake, 2020. Overcoming nonstructural protein 15-nidoviral uridylate-specific endoribonuclease (nsp15/NendoU) activity of SARS-CoV-2. Future. Drug Discov. FDD42. https://doi.org/10.4155/fdd-2020-0012.

Sohrabi, C., Alsafi, Z., O'Neill, N., Khan, M., Kerwan, A., Al-Jabir, A., Iosifidis, C., Agha, R., 2020. World Health Organization declares global emergency: a review of the 2019 novel coronavirus (COVID-19). Int. J. Surg. 71–76. https://doi.org/10.1016/j.ijsu.2020.02.034.

Song, Z., Xu, Y., Bao, L., Zhang, L., Yu, P., Qu, Y., Zhu, H., Zhao, W., Han, Y., Qin, C., 2019. From SARS to MERS, thrusting coronaviruses into the spotlight. Viruses 11 (1), 59. https://doi.org/10.3390/v11010059.

Stoermer, M., 2020. Homology models of the papain-like protease PLpro from coronavirus 2019-nCoV ChemRxiv. http://doi.org/10.26434/chemrxiv.11799705.v1.

Wang, L., Wang, Y., Ye, D., Liu, Q., 2020a. Review of the 2019 novel coronavirus (SARS-CoV-2) based on current evidence. Int. J. Antimicrob. Agents 56 (3), 105948. https://doi.org/10.1016/j.ijantimicag.2020.105948.

Wang, M., Cao, R., Zhang, L., Yang, X., Liu, J., Xu, M., Shi, Z., Hu, Z., Zhong, W., Xiao, G., 2020b. Remdesivir and chloroquine effectively inhibit the recently emerged novel coronavirus (2019-nCoV). in vitro. Cell Res. 30 (3), 269–271. https://doi.org/10.1038/s41422-020-0282-0.

Wu, F., Zhao, S., Yu, B., Chen, Y.M., Wang, W., Song, Z.G., Hu, Y., Tao, Z.W., Tian, J.H., Pei, Y.Y., Yuan, M.L., Zhang, Y.L., Dai, F.H., Liu, Y., Wang, Q.M., Zheng, J.J., Xu, L., Holmes, E.C., Zhang, Y.Z., 2020. A new coronavirus associated with human

respiratory disease in China. Nature 579 (7798), 265–269. https://doi.org/10.1038/s41586-020-2008-3.

Yang, Z., Lasker, K., Schneidman-Duhovny, D., Webb, B., Huang, C.C., Pettersen, E.F., Goddard, T.D., Meng, E.C., Sali, A., Ferrin, T.E., 2012. UCSF Chimera, MODELLER, and IMP: an integrated modeling system. J. Struct. Biol. 179 (3), 269–278. https://doi.org/10.1016/j.jsb.2011.09.006.

Zhang, X.W., Yap, Y.L., 2004. Old drugs as lead compounds for a new disease? Binding analysis of SARS coronavirus main proteinase with HIV, psychotic and parasite drugs. Bioorg. Med. Chem. 12 (10), 2517–2521. https://doi.org/10.1016/j.bmc.2004.03.035.